

## MECHANISM AND ATOMIC STRUCTURE OF SUPEROXIDE DISMUTASE

VICTORIA A. ROBERTS, CINDY L. FISHER, SUSAN M. REDFORD,  
DUNCAN E. MCREE, HANS E. PARGE, ELIZABETH D. GETZOFF and  
JOHN A. TAINER

*Department of Molecular Biology, Research Institute of Scripps Clinic, La Jolla,  
California 92037, USA*

The active site Cu ion in Cu,Zn superoxide dismutase is alternately oxidized and reduced during the enzymatic dismutation of superoxide to hydrogen peroxide and molecular oxygen. For oxidized Cu,Zn superoxide dismutase, an atomic structure has been determined for the human enzyme at 2.5 Å resolution. The resolution of the bovine enzyme structure has been extended to 1.8 Å. Atomic resolution data has been collected for reduced and inhibitor-bound Cu,Zn superoxide dismutases, and the interpretation of the electron density difference maps is in progress. The geometry and molecular surfaces of the active sites in these structures, together with biochemical data, suggest a specific model for the enzyme mechanism. Similarities in the active site geometry of the Mn and Fe superoxide dismutases with the Cu,Zn enzyme suggest that dismutation in these enzymes may follow a similar mechanism.

KEY WORDS: Superoxide dismutase, enzyme structure, enzyme mechanism.

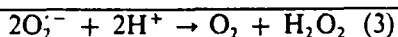
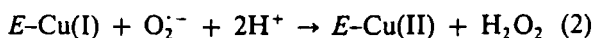
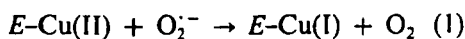
Superoxide dismutases are ubiquitous enzymes in oxygen-tolerant organisms. A family of superoxide dismutase (SOD) enzymes having Cu and Zn (Cu,Zn SOD) or either Mn (Mn SOD) or Fe (Fe SOD) at the active site protect the organism against the toxic effects of the superoxide radical ( $O_2^{\cdot -}$ ) by catalyzing its dismutation to molecular oxygen and hydrogen peroxide; this reaction occurs through the alternate reduction and oxidation of the active site metal ion (Cu, Mn, or Fe), giving the overall reaction:  $O_2^{\cdot -} + O_2^{\cdot -} + 2H^+ \rightarrow H_2O_2 + O_2$ .<sup>1</sup>

A full understanding of enzymatic activity requires a detailed knowledge of the structure at a level that approaches atomic resolution. Due to its biochemical properties and activity, SOD has been widely studied using a broad spectrum of techniques, including x-ray crystallography. The three-dimensional x-ray structures of Cu,Zn SOD,<sup>2-4</sup> Fe SOD,<sup>5</sup> and Mn SOD<sup>6</sup> have contributed directly to understanding both the activity and biochemical properties of SODs, and have provided specific models for further investigations of these enzymes. Studies using structural information from crystallography in combination with computational and biochemical results have brought an increased understanding of the mechanism and activity of SODs.

The superoxide radical is unstable in an aqueous environment and spontaneously dismutates to  $O_2$  and  $H_2O_2$ . At pH 7.4, the rate of spontaneous dismutation is about  $2 \times 10^5 \text{ M}^{-1} \text{ sec}^{-1}$ .<sup>7</sup> The uncatalyzed dismutation involves the direct reaction of two superoxide molecules, but is hindered by electrostatic repulsion between the two anions. The *in vivo* dismutation rate without catalysis is also affected by the low steady state concentration of superoxide ( $10^{-10} \text{ M}$ ).<sup>7</sup> SOD solves these problems by the alternate reduction and oxidation of the enzyme during successive encounters with

superoxide, thereby catalyzing electron transfer between two  $O_2^-$  anions without requiring their direct interaction. Comparison of the rate constant for the spontaneous dismutation<sup>7</sup> with that for the enzymatic reaction<sup>8</sup> indicates that, at physiological pH, the Cu,Zn SOD enzyme increases the rate over noncatalyzed  $O_2^-$  breakdown about 10,000 fold.

The equation for the mechanism of Cu,Zn SOD catalysis has been determined by pulse radiolysis.<sup>8-10</sup> The enzyme thus undergoes a reduction and reoxidation of the active site Cu via a two-step catalysis:



### ATOMIC STRUCTURE OF CU,ZN SOD

The structure of bovine Cu,Zn SOD with Cu(II) has been solved to an *R*-factor of 0.14, which suggests a positional error of less than 0.2 Å for atoms in the active site around the metal ions.<sup>2</sup> The resolution of this structure has been extended to 1.8 Å. The structure of the oxidized human Cu,Zn SOD enzyme has been determined at 2.5 Å resolution and is consistent with the structural features seen in the bovine enzyme. Cu,Zn SOD is a dimer made up of two identical single domain subunits of the antiparallel  $\beta$  category.<sup>3</sup> The two identical subunits of the dimer are related by a noncrystallographic twofold axis that orients the two active sites facing away from each other with the Cu atoms 33.8 Å apart. Each 16,000 dalton subunit (151 amino acid residues) is composed of eight antiparallel  $\beta$  strands, which form a flattened cylinder, plus three external loops. The SOD  $\beta$  barrel structure consists of four very regular, extended  $\beta$  strands on one side and four  $\beta$  strands in more twisted or irregular conformations on the other side. The two sides of the  $\beta$  barrel might also be interpreted as two  $\beta$  sheets forming a sandwich. The loops contain tight turns and are primarily as well-defined and ordered as the  $\beta$  strands. The active site, which contains one Cu and one Zn ion, is made of two large loops that connect the  $\beta$  strands. The single disulfide bridge forms a left-handed spiral conformation and ties one loop to the  $\beta$  barrel. Within the major category of antiparallel  $\beta$  domains, the overall topology of the SOD subunit classifies the enzyme as a Greek-key  $\beta$  barrel.

The geometry of the active site metals of bovine Cu,Zn SOD and their ligands in the oxidized enzyme, as viewed from the solvent, is shown in Figure 1.<sup>2</sup> The active site copper ion, which is alternately oxidized and reduced during the enzymatic reaction, is ligated by the imidazole nitrogens of four histidine residues: ND1 (the proximal N) of His 44, and NE2 (the distal N) of His 46, 61, and 118. The arrangement and orientation of these histidine ligands make the axial position of the Cu much more open on the solvent side than on the protein side, allowing the possibility of ligation of a solvent molecule with the metal. A solvent peak in the fragment difference map ( $F_o - F_c$ ), representing electron density not accounted for by the protein, is located about 2.5 Å from the Cu(II), suggesting that a water molecule is coordinated to the axial position. Difference maps also show other peaks in the active site channel near the Cu ion consistent with a network of hydrogen-bonded water molecules. The

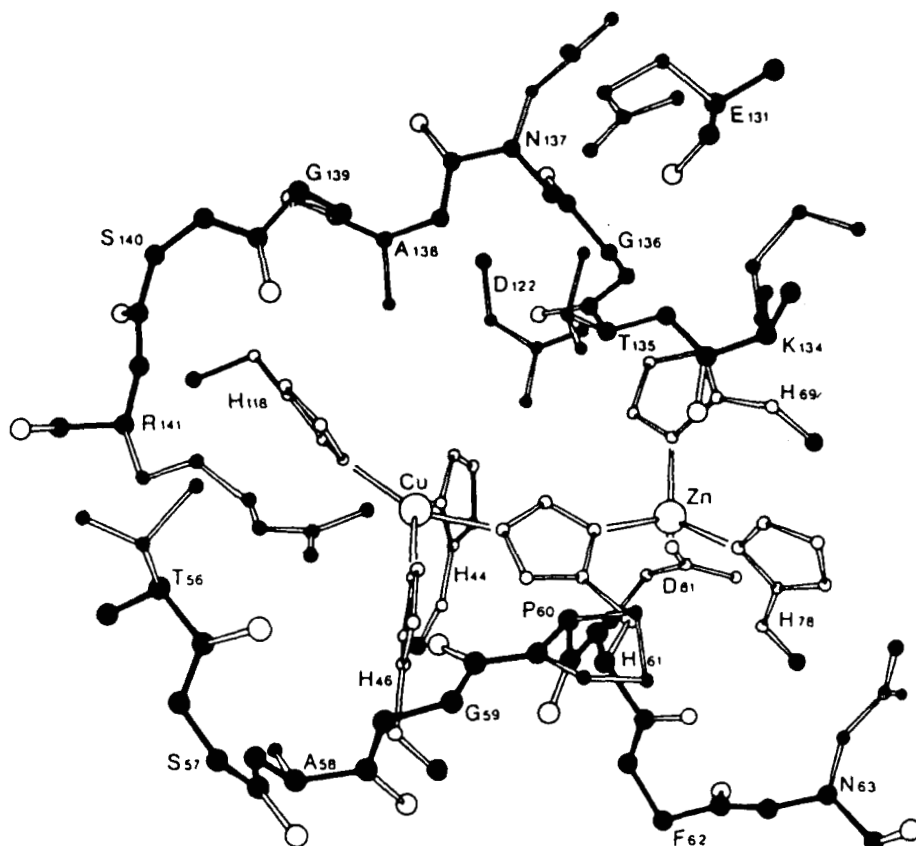


FIGURE 1. Critical active site channel residues of SOD as viewed from the solvent. The main chain is shown by solid black bonds and atoms, the ligand side chains by open bonds and atoms, and the other side chains by solid atoms and open bonds. Main-chain atoms only of residues 57, 62, and 140 have also been included in the drawing for continuity. (Adapted from Tainer *et al.*<sup>4</sup>)

existence of at least one water bound to the Cu has also been indicated by NMR data.<sup>11</sup>

The Zn ion is ligated by three histidines and one oxygen from the side chain of Asp 81.<sup>2</sup> His 61, 69, and 78 all ligate the Zn(II) with ND1 (the proximal N). The Zn ligand geometry is tetrahedral with a strong distortion toward a trigonal pyramid with Asp 81 at the apex. The three histidine rings are located slightly in front of the Zn in the direction of the active channel, with Asp 81 behind and completely buried.

A unique aspect of Cu,Zn SOD is the bridge formed by ligand His 61 between the copper and zinc ions, with the imidazole ring approximately planar to both metals. The metal ligand geometry and the histidine ring orientations are clearly seen in the high resolution x-ray structure. In the oxidized Cu,Zn SOD structure, His 61 bridges between the Cu and Zn metal atoms at the crystallization pH of 7.5. Spectrophotometric data of the oxidized enzyme suggest that this bridge remains unbroken over the pH range from 5 to 9.5 in which Cu,Zn SOD activity level is constant.<sup>9</sup> Hodgson and

Fridovich<sup>12</sup> have postulated that this bridging His imidazolate ring may function as a proton carrier to facilitate protonation of the  $O_2^-$  that interacts with the reduced enzyme.

Active site area of Cu,Zn SOD is made up of highly conserved, closely packed residues.<sup>4</sup> The active site Cu(II) and Zn(II) ions lie 6.3 Å apart at the bottom of a long channel between two large loop regions on the external surface of  $\beta$  barrel strands 5e, 6d, and 7g. Twenty-one residues contribute to the active site channel structure (Figure 1). Residues Glu 131, Lys 134, Thr 135, Gly 136, Asn 137, Ala 138, Gly 139, and Arg 141 form one rim of the channel and residues Thr 56, Ala 58, Gly 59, Pro 60, and Asn 63 form the other rim. The metals and their seven ligating residues form the floor of the channel with Asp 122 buried beneath. Compared with the rest of the molecule, the residues of the channel are highly conserved in the published sequences of Cu,Zn SODs,<sup>13</sup> suggesting that the topography of the channel's surface is critical to the enzymes' function.<sup>4</sup> This channel is shaped like a funnel, wide at the outside, and narrowing down as it leads inward to the Cu ion (see Figure 2).

The molecular orientations of both the side chains and the main chains of the Cu- and Zn-ligating residues are stabilized by an interlocked network of hydrogen bonds. The positions of the ligand side chains are also stabilized by extensive nonbonded contacts. These hydrogen-bonding and tight packing interactions in the active channel suggest that, regardless of any possible strain implied by distortions of the metal-ligand geometry, large movements or rearrangements of the ligands during catalysis are unlikely. The two metal ions in each subunit interact directly through His 61 and indirectly through a hydrogen bond network involving Asp 122, which forms hydrogen bonds to the Cu ligand His 44 and the Zn ligand His 69. The low temperature factors (suggesting little local mobility) and clear definition in the electron density maps of the active site channel residues are consistent with this area being quite stable and ordered without significant dynamic or static structural variations.

The surface of the active channel comprises approximately 610 Å<sup>2</sup> or about 10% of the total exposed surface area. The Cu(II) ion exposes about 5 Å<sup>2</sup> of its surface area to the probe, but the Zn(II) ion is completely buried. There are two pits forming specific binding sites in the floor of the active channel. The Cu pit is located directly above the Cu(II) and involves the Cu ion, His 61, His 118, Thr 135, and Arg 141; the water pit is adjacent to this position above and between the Cu ligands His 44 and 118

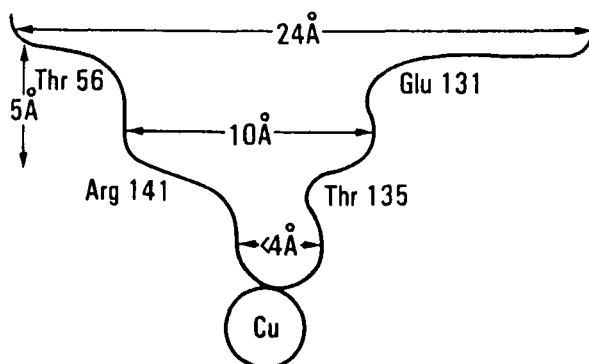


FIGURE 2. Schematic view of the shape and dimensions of the active site channel in cross-section. The amino acids forming the channel wall are indicated. Lys 134, located forward of the plane of the paper and adjacent to Glu 131, also contributes structurally to channel architecture.

and is surrounded by Thr 135, Gly 136, Ala 138, and Gly 139. Both pits lie in the particularly narrow part of the channel between the guanidinium group of Arg 141 and the side chain of Thr 135 (see Figure 2). The Cu pit is complementary to superoxide and would place the superoxide molecule in the proper geometry to interact directly with the copper. Thus, the high resolution structure of bovine Cu,Zn SOD presents a picture of an enzyme that has developed to fit its substrate optimally in the active site.

MECHANISM OF SOD AS SUGGESTED BY THE CRYSTAL STRUCTURE

If  $O_2^-$  does bind directly to the Cu, as implied by the perfect fit of a superoxide into the pit above the Cu(II), what active site geometry would result during the different steps in the reaction equation? When the  $O_2^-$  binds, there is a virtual shift in the mean ligand plane so that  $O_2^-$  binding is equatorial. One superoxide oxygen atom binds to the positively charged Cu(II) while the other oxygen atom is positioned to form a hydrogen bond with the positively charged guanidinium nitrogen on Arg 141 (Figure 3). Bound  $O_2^-$  reduces the Cu(II) to Cu(I) with the simultaneous breaking of the bond between His 61 and the Cu ion, and  $O_2$  is released. The His 61 side chain is forced out of the plane of the two metals, allowing a more tetrahedral geometry around the Zn(II), and protonated. Once the Zn(II) has relaxed to this geometry, the hydrogen on His 61 NE2 is in a perfect position for donation to the second superoxide anion.

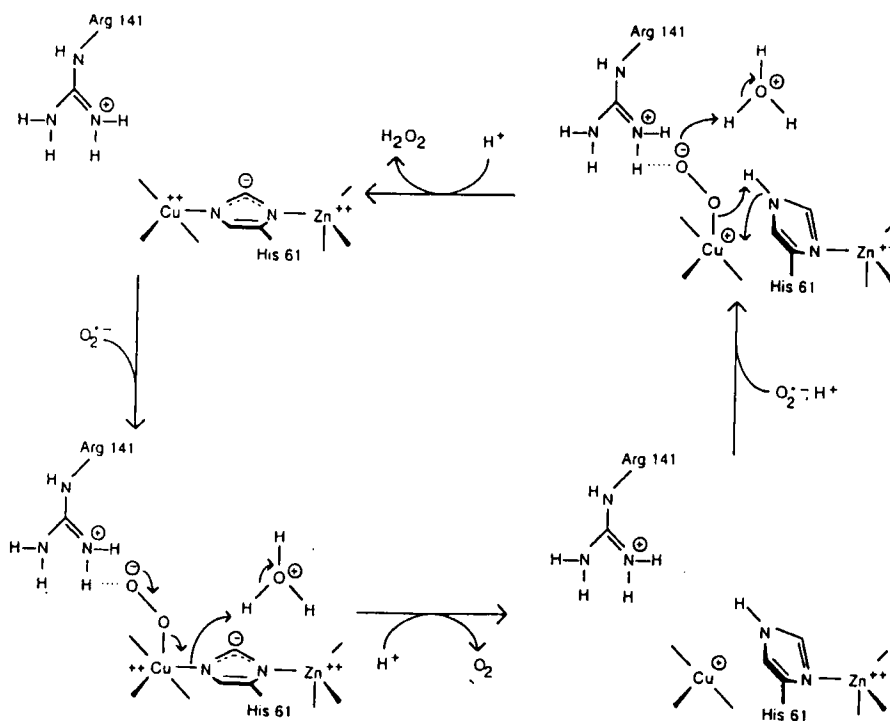


FIGURE 3. Schematic mechanism of the oxidation-reduction pathway in Cu,Zn SOD.

Free Radic Res Downloaded from informahealthcare.com by Library of Health Sci- Univ of Il on 11/08/11  
For personal use only.

The total movement of His 61 need not be large; a rotation about the  $C_{\beta}$ - $C_{\gamma}$  bond is sufficient to move His 61 NE2 out of the plane of the metals about 0.6 Å. Further movements around the Cu site during reduction, such a shift in the position of His 44, might be transmitted through the Asp 122 hydrogen-bond bridge to reduce distortion of the Zn site also.

Binding of a second  $O_2^-$  directly to the Cu(I) ion places one superoxide oxygen atom in position to form a short, charged hydrogen bond to the hydrogen atom on His 61 NE2, while the second oxygen atom of superoxide can still be positioned to form a hydrogen bond to the positively charged Arg 141 guanidinium group, as in the first step of catalysis (Figure 3). While His 61 ND1 is bound to the Zn(II) ion but not to the Cu(I) ion, the  $pK_a$  for the dissociation of the proton on NE2 is above 9,<sup>14</sup> so NE2 will always be protonated at physiological pH. Based upon the superoxide coordinates from docking  $O_2^-$  into the best fit in the active site, the distance from rotated His 61 NE2 to the nearer superoxide oxygen atom is about 2.5 Å, which is consistent with a charged hydrogen bond involving partial proton transfer to the superoxide.<sup>15,4</sup> The proton is transferred to the superoxide with spontaneous oxidation of the Cu and reformation of the bond between His 61 and the Cu, resulting in production of a hydrogen peroxide molecule. This inner-sphere mechanism, proposed from implications from the x-ray structure of the Cu,Zn enzyme, suggests a catalytic role for the Zn,<sup>4</sup> in addition to the previously proposed structural role.<sup>16</sup> In the first step of the dismutation reaction, relaxation of the distortions in the Zn-ligand geometry present in the Cu(II) enzyme (mediated through the His 61 imidazolate bridge and the pair of hydrogen bonds to Asp 122) may stabilize the transition state. In the second step of the reaction, the roles of the Zn are to assure protonation of His 61 NE2 and to position this proton correctly for hydrogen-bonding and subsequent transfer to the second incoming  $O_2^-$ , thus completing the catalytic cycle. The Zn would enhance the enzymatic activity without being essential, since His 61 NE2 will be at least partially protonated at pH 7 and the necessary protons are also available from the water molecules in the active channel.

The very fast rate of the reaction implies that no large rearrangements of the active site can occur during the reaction. All of the movements discussed above – the breaking of histidine bond to the Cu ion and the corresponding rearrangements of the ligands around the metals upon reduction – involve small movements, mainly rotations, of the histidine rings.

### *Evidence for Mechanism*

We have solved the structure of the Cu(I) enzyme, and have found it to be consistent with the above mechanism. Comparison of the electron density maps for the reduced and oxidized bovine SODs revealed that the His 61 side chain ring has rotated. In the reduced structure, the NE2 atom, which was bound to the copper atom in the Cu(II) enzyme, now extends into the pocket of the active site. Spectral and kinetic evidence support the breaking of the His 61-Cu bond during the enzymatic catalysis,<sup>17</sup> causing the uncoupling of the metal sites<sup>18</sup> and the uptake of one proton per subunit<sup>19</sup> by the His 61 ring nitrogen not ligated to the Zn(II).<sup>20</sup> The removal of the His 61 imidazole nitrogen from the Cu coordination changes the Zn(II) x-ray absorption spectrum<sup>21</sup> and the visible spectrum of the Co in the Zn site of Cu(I)<sub>2</sub>Co(II)<sub>2</sub> derivatives,<sup>22</sup> indicating coupling of the Cu ionization state to the Zn-ligand geometry. The proton NMR spectrum of the Cu(I)<sub>2</sub>Co(II)<sub>2</sub> derivative<sup>23</sup> shows that all three histidine residues

ligated to the Zn ion each have one exchangeable proton, which indicates that the His 61 bond to the Cu(I) must be broken and His 61 be protonated in the reduced enzyme. X-ray absorption spectroscopy suggests that the Cu site becomes more tetrahedral upon reduction.<sup>21</sup>

### *Binding of Anion Inhibitors*

Examination of a complex of SOD with superoxide has been impossible because the rate of reaction is so great. The binding of several anion inhibitors of Cu,Zn SOD has been examined in the hopes of learning more about the mechanism. For the Cu(II) enzyme,  $\text{CN}^-$ ,  $\text{N}_3^-$ ,  $\text{SCN}^-$ ,  $\text{OCN}^-$ , and halides are reported to bind to the copper.<sup>24-26</sup> The narrow width of the active site channel ( $< 4 \text{ \AA}$ ) just above the Cu ion (Figure 2) is consistent with the accessibility of the Cu to  $\text{Cl}^-$  (diameter of  $3.62 \text{ \AA}$ ) and  $\text{Br}^-$  (diameter of  $3.90 \text{ \AA}$ ), but not  $\text{I}^-$  (diameter of  $4.32 \text{ \AA}$ ).<sup>27</sup> The competitive anion inhibitors ( $\text{CN}^-$ ,  $\text{N}_3^-$ , and  $\text{F}^-$ ) apparently bind by displacing a water molecule,<sup>28</sup> as was proposed for  $\text{O}_2^-$  binding from the atomic structure of the Cu,Zn enzyme.<sup>4</sup>

Cyanide binds reversibly in a one-to-one ratio with the Cu(II) ion<sup>10</sup> to inhibit Cu,Zn SOD.<sup>29</sup> ESR studies of the  $^{13}\text{CN}^-$ -enzyme complex indicate that cyanide binds equatorially<sup>24,30,31</sup> with the carbon atom bound to the Cu(II).<sup>31</sup> The ESR spectrum of the enzyme with  $\text{CN}^-$  bound is also more axial, suggesting a less distorted Cu ion geometry than in the native enzyme alone. These data have been interpreted to indicate that cyanide promotes a major reorganization of the Cu(II) ligands, including displacement of a histidine ligand.<sup>16,32,33</sup> Currently, electron spin echo studies suggest that, contrary to earlier proposals, the His imidazole bridge between the Cu(II) and the Zn(II) remains intact on binding both  $\text{CN}^-$  and  $\text{N}_3^-$ .<sup>16,32</sup> Instead, either His 44 or 46 is thought to be displaced when  $\text{CN}^-$  binds. The ligand geometry and lack of solvent accessibility of these two histidines make it unlikely that there is large rearrangement of these tightly packed residues by  $\text{CN}^-$ .

Based upon the geometry and molecular surface obtained from the crystal structure, it is clear that replacement of the axial water by a stronger ligand could allow a virtual rearrangement of the mean equatorial plane, such that the solvent-accessible binding position becomes part of the new equatorial plane.<sup>4</sup> Therefore, a  $\text{CN}^-$  ion could bind in either the superoxide anion site or the water site, and shift the equatorial plane without allowing electron transfer. As a result of this virtual rearrangement, the Cu site geometry would be more axial, as observed by ESR, because the new equatorial plane is less distorted. In this model His 46 or His 44 becomes axial, with only small movements required. The axial-equatorial interconversion model for anion binding to Cu,Zn SOD explains the data on anion inhibitors without requiring the large physical rearrangements in the active site that others have proposed.<sup>34,35</sup>

NMR studies on  $\text{Cu(II)}_2\text{Co(II)}_2\text{SOD}$ <sup>36,37</sup> validate the axial-to-equatorial interconversion for anion binding. Very large shifts of the resonances due to either His 44 or His 46 from the paramagnetic region to the diamagnetic region are seen as azide is bound.<sup>36,37</sup> The relaxation times<sup>37</sup> revealed very small movements of the His ligand, predominantly a rotation about the  $\text{C}_\beta\text{-C}_\gamma$  bond. Thus, the anion binding causes a change in the mean equatorial plane of ligands around the Cu ion, but with little movement in this tightly packed region of the protein.

To ascertain the precise movements in the active site, we have solved and are currently analyzing the structure of Cu(II) bovine SOD with cyanide bound. Preliminary examination of the electron density reveals that the bond between His 61 and the

Cu ion is retained and that the other Cu ligands have undergone small changes in position relative to the native structure. The cyanide anion binds in the Cu pit, the hypothetical superoxide binding site, replacing the water seen in the native structure.

## COMPARISON WITH FE AND MN SODS

The overall structure of the Fe and Mn enzymes is very different from that determined for the Cu,Zn enzyme. The Fe/Mn SODs are either dimeric or tetrameric and composed of subunits with molecular weights of about 20,000 (180 to 200 amino acids) and one Mn or one Fe each.<sup>38</sup> X-ray structures of Fe SOD<sup>5,39</sup> show a fold with over 50% helicity. The structure of Mn SOD from *T. thermophilus*<sup>40</sup> indicates a helical fold closely analogous to that of Fe SOD, with equivalent metal and ligand positions. Despite these large differences in overall structure compared with the Cu,Zn enzyme, the active sites of the Fe and Mn enzymes appear to resemble the Cu,Zn enzyme. In the oxidized Mn SOD, the ligands have a distorted trigonal pyramidal geometry around the Mn. His 28 and a water molecule are the apical ligands with His 83, His 170, and Asp 166 making up the rest of the pentacoordinate complex.<sup>6</sup> Although the Fe SOD sequence information is incomplete, rigid-body transformations of the Mn SOD model onto the Fe SOD electron density maps show that the Fe SOD ligand geometry closely matches the pentacoordinate geometry seen for Mn SOD.<sup>41-43</sup> Using a partial sequence for Fe SOD from *P. ovalis*, it has been determined that three of the ligands are two histidines corresponding to His 28 and His 170 in the Mn SOD structure and one is an aspartate corresponding to Asp 166.<sup>42</sup> The structure is not sufficiently resolved to see a water ligand, but NMR indicates a water ligand to the Fe does exist.<sup>44</sup> The geometries of the Fe and Mn enzymes thus show similarities to the Cu,Zn enzyme in at least three respects: 1) four protein side chains act as metal ligands, 2) a single water molecule makes a fifth metal ligand, and 3) the overall geometry places the water molecule and a protein side chain in trans positions (His 44 could be described as being trans to the axial water ligand in Cu,Zn SOD). Thus, the general arrangement of the ligands in all three enzymes could be described as a tetrahedral distortion from a square plane of protein ligands with an axial water ligand. The similarity of the general arrangement of ligands in the active site and surrounding side chains indicates that Fe and Mn SODs catalysis may involve a mechanism similar to that proposed for Cu,Zn SOD. Detailed information is available on the active site environment for the Mn SOD from *T. thermophilus*.<sup>6</sup> As in Cu,Zn SOD, the active site ligands are held in their orientations by a combination of hydrogen-bonding and packing interactions. In addition to the ligands, a group of aromatic side chains, including Tyr 36, Phe 86, Trp 132, and Trp 168, are positioned within 7 Å of the Mn ion and five additional aromatic side chains (His 32, His 33, Trp 87, Tyr 172, and Tyr 183) are only slightly farther away. Six of these aromatic side chains (Tyr 36, Phe 86, Trp 87, Trp 132, Trp 168, and Tyr 183) provide a tightly packed hydrophobic lining around most of the metal-ligand center.

## SUMMARY

Comparison of spectroscopic, NMR, ESR, and other physical techniques with the crystallographic structures has resulted in a detailed molecular mechanism for



superoxide dismutase catalysis. The oxidized, the reduced, and the cyanide bound bovine Cu,Zn SOD structures have confirmed and provided details for the mechanism involving the breaking and reforming of the bond between the Cu ion and His 61. A catalytic role for the Zn ion in positioning the imidazole ring of His 61 has been demonstrated by the reduced structure. The cyanide bound structure confirms the binding site for the superoxide radical anion. Comparison of bovine Cu,Zn SOD with human Cu,Zn SOD has confirmed that the shape of the active site including the geometry of the His ligands and the active site channel are completely conserved. The geometry of the active site ligands is conserved not only for the Cu,Zn SODs from different species, but also in the Fe and Mn SODs.

### Acknowledgments

This work was funded in part by the National Institutes of Health Grants GM 39345 (to J.A.T) GM 37684 (to E.D.G), and fellowship GM11612 to (C.L.F.).

### References

1. I. Fridovich (1979) *Superoxide and Superoxide Dismutase*; Elsevier/North Holland: New York, pp 67-90.
2. J.A. Tainer, E.D. Getzoff, K.M. Beem, J.S. Richardson and D.C. Richardson (1982) *Journal of Molecular Biology*, **160**, 181-217.
3. E.D. Getzoff, J.A. Tainer, P.K. Weiner, P.A. Kollman, J.S. Richardson and D.C. Richardson (1983) *Nature*, **306**, 287-290.
4. J.A. Tainer, E.D. Getzoff, J.S. Richardson and D.C. Richardson (1983) *Nature*, **306**, 284-287.
5. W.C. Stallings, T.B. Powers, K.A. Patridge, J.A. Fee and M.L. Ludwig (1983) *Proceedings of the National Academy of Sciences U.S.A.* **80**, 3884-3888.
6. W.C. Stallings, K.A. Patridge, R.K. Strong and M.L. Ludwig (1985) *Journal of Biological Chemistry*, **260**, 16424-16432.
7. I. Fridovich (1975) *Annual Review of Biochemistry*, **44**, 147-159.
8. D. Klug-Roth, I. Fridovich and J. Rabani (1973) *Journal of the American Chemical Society*, **95**, 2786-2790.
9. D. Klug, J. Rabani and I. Fridovich (1972) *Journal of Biological Chemistry*, **247**, 4839-4842.
10. G. Rotilio, R.C. Bray and E.M. Fielden (1972) *Biochimica et Biophysica Acta*, **268**, 605-609.
11. B.P. Gaber, R.D. Brown, S.H. Koenig and J.A. Fee (1972) *Biochimica et Biophysica Acta*, **271**, 1-5.
12. E.K. Hodgson and I. Fridovich (1975) *Biochemistry*, **14**, 5294-5303.
13. G. Steffens, E. Frankus, K. Hering, S.M.A. Kim, F. Ötting, E. Schwertner, K. Puget, A.M. Michelson and L. Flohe (1986) *Sequencing Confirms Normal Divergent Evolution of Cu/Zn SOD*; Elsevier Science: Amsterdam, pp 246-248.
14. R.J. Sundberg and R.B. Martin (1974) *Chemical Reviews*, **74**, 471-517.
15. J.D. Stoesz, D.P. Malinowski and A.G. Redfield (1979) *Biochemistry* **18**, 4669-4675.
16. J.S. Valentine and M.W. Pantoliano (1981) *Protein-Metal Ion Interactions in Cuprozinc Protein (Superoxide Dismutase), a Major Intracellular Repository for Copper and Zinc in the Eukaryotic Cell*; John Wiley and Sons: New York, Vol. 3, pp 291-358.
17. M.E. McAdam, E.M. Fielden, F. Lavelle, L. Calabrese, D. Cocco and G. Rotilio (1977) *Biochemical Journal*, **167**, 271-274.
18. G. Rotilio, L. Calabrese, B. Mondovi and W.E. Blumberg (1974) *Journal of Biological Chemistry*, **249**, 3157-3160.
19. G.D. Lawrence and D.T. Sawyer (1979) *Biochemistry*, **18**, 3045-3050.
20. L. Morpurgo, G. Giovagnoli and G. Rotilio (1973) *Biochimica et Biophysica Acta*, **322**, 204-210.
21. W.E. Blumberg, J. Peisach, P. Eisenberger and J.A. Fee (1978) *Biochemistry*, **17**, 1842-1846.
22. J.A. Fee and W.D. Phillips (1975) *Biochimica et Biophysica Acta*, **412**, 26-38.
23. I. Bertini, C. Luchinat and R. Monnanni (1985) *Journal of the American Chemical Society*, **107**, 2178-2179.
24. G. Rotilio, A. Finazzi Agro, L. Calabrese, F. Bossa, P. Guerrieri and B. Mondovi (1971) *Biochemistry*, **10**, 616-621.

25. J.A. Fee and B.P. Gaber (1972) *Journal of Biological Chemistry*, **247**, 60–65.
26. A. Rigo, P. Viglino, L. Calabrese, D. Cocco and G. Rotilio (1977) *Biochemical Journal*, **161**, 27–30.
27. A. Rigo, R. Stevanato, P. Viglino and G. Rotilio (1977) *Biochemical and Biophysical Research Communications*, **79**, 776–783.
28. N. Boden, M.C. Holmes and P.F. Knowles (1979) *Biochemical Journal*, **177**, 303–309.
29. G. Rotilio, L. Calabrese, F. Bossa, D. Barra, A. Finazzi Agro and B. Mondovi (1972) *Biochemistry*, **11**, 2182–2187.
30. G. Rotilio, L. Morpurgo, C. Giovagnoli, L. Calabrese and B. Mondovi (1972) *Biochemistry*, **11**, 2187–2192.
31. P.H. Haffner and J.E. Coleman (1973) *Journal of Biological Chemistry*, **248**, 6626–6629.
32. J.A. Fee, R.A. Lieberman, H. Van Camp, J. Peisach and W.B. Mims (1980) *Federation Proceedings* **39**, 1769.
33. R.A. Lieberman (1981) Ph.D. Thesis, University of Michigan, Ann Arbor, MI.
34. R.A. Lieberman, R.H. Sands and J.A. Fee (1982) *Journal of Biological Chemistry*, **257**, 336–344.
35. H.L. Van Camp, R.H. Sands and J.A. Fee (1982) *Biochimica et Biophysica Acta*, **704**, 75–89.
36. I. Bertini, G. Lanini, C. Luchinat, L. Messori, R. Monnanni and A. Scozzafava (1985) *Journal of the American Chemical Society* **107**, 4391–4396.
37. L. Banci, I. Bertini, C. Luchinat and A. Scozzafava (1987) *Journal of the American Chemical Society*, **109**, 2328–2334.
38. M.L. Ludwig, K.A. Patridge and W.C. Stallings (1986) *Manganese Superoxide Dismutase: Structure and Properties*; Academic: Orlando, pp 405–430.
39. D. Ringe, G.A. Petsko, F. Yamakura, K. Suzuki and D. Ohmori (1983) *Proceedings of the National Academy of Sciences U.S.A.* **80**, 3879–3883.
40. W.C. Stallings, K.A. Patridge, R.K. Strong and M.L. Ludwig (1984) *Journal of Biological Chemistry*, **259**, 10695–10699.
41. W.C. Stallings, C. Bull, K.A. Patridge, T.B. Powers, J.A. Fee, M.L. Ludwig, D. Ringe and G.A. Petsko (1984) *The Three-Dimensional Structure of Iron Superoxide Dismutase: Kinetic and Structural Comparisons with Cu/Zn and Mn Dismutases*; Walter de Gruyter: Berlin, pp. 779–792.
42. W.C. Stallings, K.A. Patridge and M.L. Ludwig (1986) *The Active Centers of T. thermophilus Mn Superoxide Dismutase and E. coli Fe Superoxide Dismutase: Current Status of the Crystallography*; Elsevier Science: Amsterdam, pp. 195–201.
43. W.C. Stallings, K.A. Patridge, R.K. Strong, M.L. Ludwig, F. Yamakura, T. Isobe and H.M. Steinman (1987) *Active Site Homology in Iron and Manganese Superoxide Dismutases*; Oxford University: Oxford, pp. 505–514.
44. J.J. Villafranca, (1976) *FEBS Letters*, **62**, 230–232.

Accepted by Prof. G. Czapski